

lisions of metastable He with Ar has been reported in the literature.<sup>6,7</sup> Moreover, in recent experiments<sup>8</sup> we noticed a strong temperature dependence of the intensity ratio  $\text{HeAr}^+/\text{Ar}^+$ , a fact which also would be expected from the electron energy distribution observed.

Much new information about the details of Reactions (1) and (3), namely about the ionization probability as a function of the separation between  $A^*$  and  $B$  and about the interaction forces before and after the ionization, is contained in electron energy distributions as shown in Figs. 1 and 2. Since no valid theory is available to extract this information, we attempt to explain the measured distributions in terms of potential energy curves of the collision system before and

after the ionization, the ionization itself being considered fast compared with the relative motion of the heavy particles. More experimental data and a detailed discussion will be published.

<sup>1</sup>A. A. Kruithof and F. M. Penning, *Physica* **4**, 430 (1937).

<sup>2</sup>V. Cermák, *J. Chem. Phys.* **44**, 3774 (1966).

<sup>3</sup>H. Hotop and A. Niehaus, to be published.

<sup>4</sup>J. L. G. Dugan, H. L. Richards, and E. E. Mushlitz, *J. Chem. Phys.* **46**, 346 (1967).

<sup>5</sup>A. L. Smith, *J. Chem. Phys.* **47**, 1561 (1967).

<sup>6</sup>M. S. B. Munson, J. L. Franklin, and F. H. Field, *J. Phys. Chem.* **67**, 1542 (1963).

<sup>7</sup>J. A. Herce, K. D. Foster, and E. E. Mushlitz, Jr., *Bull. Am. Phys. Soc.* **13**, 206 (1968).

<sup>8</sup>H. Hotop and A. Niehaus, to be published.

### BRUECKNER-GOLDSTONE MANY-BODY THEORY FOR THE HYPERFINE STRUCTURE OF PHOSPHORUS\*

N. C. Dutta, C. Matsubara, R. T. Pu, and T. P. Das  
Department of Physics, University of California, Riverside, California

(Received 25 July 1968)

The Brueckner-Goldstone many-body perturbation theory is utilized to study the hyperfine interaction in atomic phosphorus. By this method, a correlation contribution to the hfs constant of a positive sign and an appropriate magnitude is obtained, which predominates over the negative core-polarization effect to produce substantial agreement with experiment.

The hyperfine structure constant in atomic phosphorus ( $3p^3; ^4S$ ) has been recently measured carefully by both atomic-beam<sup>1</sup> and optical-pumping<sup>2</sup> techniques to be  $A = +55.055\,691 \pm 0.000\,007$  Mc/sec. In contrast, unrestricted Hartree-Fock (UHF) and related approaches<sup>3</sup> all lead to a negative sign with values ranging from  $-42$  Mc/sec to  $-132$  Mc/sec. This sharp disagreement between theory and experiment has led to some doubts concerning the validity of the UHF procedure and, indeed, the core-polarization concept in general.<sup>3</sup> It is the purpose of the present note to present the results of a Brueckner-Goldstone-type<sup>4</sup> (BG) calculation of the hfs in atomic phosphorus, which shows that a proper treatment of correlation effects provides the requisite positive contribution which in combination with the negative core-polarization effect leads to a good agreement between theory and experiment with respect to both magnitude and sign.

The BG procedure has earlier been successfully applied to the hfs calculations of He ( $^3S$ ),<sup>5</sup> Li ( $^2S$  ground state<sup>6</sup> and  $^2P$  excited state<sup>7</sup>), and the nitrogen atom<sup>8</sup> ( $^4S$ ). The advantages of the BG

procedure for the study of hfs effects are manifold. First, being a perturbation theory, it handles small numbers rather than differences of large numbers as one does in conventional UHF calculations, where the difference of large up- and down-spin densities are evaluated.<sup>3,8</sup> Further, the technique allows a convenient separation of physical effects such as core polarization, consistency, and various types of correlation, and permits a systematic handling of such effects through diagrammatic field-theoretical technique. These advantages, plus its success with the light atoms, particularly nitrogen,<sup>9</sup> where one had a similar uncertainty in the theoretical situation in the magnitude of  $A$ , though not in sign, prompted us to apply this procedure to the phosphorus atom.

Since the BG procedure, both in its application to the hfs<sup>5-8,10,11</sup> problem as well as to other properties<sup>12</sup> of atoms, has been discussed elaborately in the past, we shall only mention a few brief facts to facilitate the description of our results.

The total Hamiltonian  $\mathcal{H}$  for the atom can be

separated into an unperturbed part,  $\mathcal{H}_0$ , and a perturbation,  $\mathcal{H}'$ , given by

$$\mathcal{H}_0 = \sum_{i=1}^N T_i + \sum_{i=1}^N V_i, \quad (1)$$

$$\mathcal{H}' = \sum_{i>j} r_{ij}^{-1} - \sum_i V_i, \quad (2)$$

where  $T_i$  is the sum of the kinetic-energy and nuclear-Coulomb-potential operators, and  $V_i$  represents the single-particle potential for the  $i$ th electron. In our calculation, we utilized the Hartree-Fock type  $V^{N-1}$  potential.<sup>12</sup> The complete orthonormal set  $\{\varphi_i\}$  of one-electron bound and continuum states is generated by solving the equation

$$(T + V)\varphi_i = \epsilon_i \varphi_i. \quad (3)$$

The  $s$  states were generated in the Hartree-Fock field of a neutral phosphorus atom with a  $3s$  electron removed. Thus, the one-electron  $3s$  state from Eq. (3) is identical with the Hartree-Fock  $3s$  state, while the  $1s$  and  $2s$  states differed slightly from the true Hartree-Fock states. The

non- $s$  states ( $p$ ,  $d$ , and  $f$ ) were generated in the field of the neutral atom minus a  $3p$  electron. The unperturbed many-electron ground state  $\Phi_0$  is given by a Slater determinant formed with the lowest  $N$  solutions  $\varphi_i$ . The true ground-state wave function  $\Psi_0$  is then given by

$$\begin{aligned} \Psi_0 &= \sum_{n=0}^{\infty} L[(E_0 - \mathcal{H}_0)^{-1} \mathcal{H}'^n \Phi_0 \\ &= |0\rangle + |1\rangle + \dots + |n\rangle + \dots + |m\rangle + \dots, \end{aligned} \quad (4)$$

where

$$E_0 = \sum_{i=1}^N \epsilon_i$$

and  $L$  denotes that only "linked" terms<sup>4</sup> are to be added. The contact hfs operator for an atom is

$$O_{\text{hfs}} = \frac{16\pi}{3} \beta \mu_N \sum_{i=1}^N \delta(\vec{r}_i) \vec{s}_i \cdot \vec{I}, \quad (5)$$

where the symbols have their usual meaning. The hfs constant  $A$  for an  $S$ -state atom is then given by

$$A = \frac{16\pi \beta \mu_N}{3} \frac{\langle \Psi_0 | \sum_{i=1}^N \delta(\vec{r}_i) s_{zi} | \Psi_0 \rangle}{\langle \Psi_0 | \Psi_0 \rangle} = \frac{16\pi \beta \mu_N}{3} \frac{\{ \langle 0 | f | 0 \rangle + \langle 0 | f | 1 \rangle + \dots + \langle m | f | n \rangle \}}{\{ \langle 0 | 0 \rangle + \langle 1 | 1 \rangle + \dots + \langle m | n \rangle + \dots \}}, \quad (6)$$

where

$$f = \sum_{i=1}^N \delta(\vec{r}_i) s_{zi}, \quad (7)$$

and  $I$  and  $S$  are the total nuclear and electronic spins. Each term in Eq. (6) can be represented by a group of Feynman-like diagrams drawn according to the rules described earlier<sup>6,8,10,12</sup> with suitable notation for hole and particle states and interaction vertices. In taking the expectation value only the linked-cluster expansion for the atomic wave function  $\Psi_0$  is used; Eq. (6) will yield some unlinked diagrams, as illustrated in Fig. 1(j). Also, Eq. (6) gives diagrams of the type Fig. 1(k), where a hfs vertex connects two different hole lines; that is,  $j \neq j'$  only. In Fig. 1, the vertex connecting wavy lines represents  $O_{\text{hfs}}$ . The downward and upward lines represent hole and particle states, respectively, while the vertex connecting dashed lines represents the interaction  $r_{12}^{-1}$ .

The most important diagrams contributing to

hfs are presented in Figs. 1(a)-1(i), and their values are listed in Table I. These values include the effect of the normalization factor in the denominator of Eq. (6), which came out to be 1.0040 including up to second order. The (0, 1) diagrams in Fig. 1(c) describe core-polarization effects. The corresponding values in Table I include the effects of hole-hole and hole-particle ladder corrections<sup>6,8,10</sup> which occur for  $1s$  and  $2s$  diagrams. The individual contributions from  $1s$ ,  $2s$ , and  $3s$  states are seen to be similar in nature and sign as in the UHF calculations, although there are differences in magnitude. Our total core-polarization result is  $-64.596$  Mc/sec, and again the negative sign is in agreement with the UHF calculation.<sup>3</sup>

The important (1, 1) diagrams in Figs. 1(b) and 1(c) represent correlation effects describable as mutual polarization of  $3p$  and  $3s$  orbitals and  $3p$  and  $2p$  orbitals. Fig. 1(c) is just the exchange counterpart of Fig. 1(b). The correlation between  $3p$  and  $3s$  was found to be much larger than

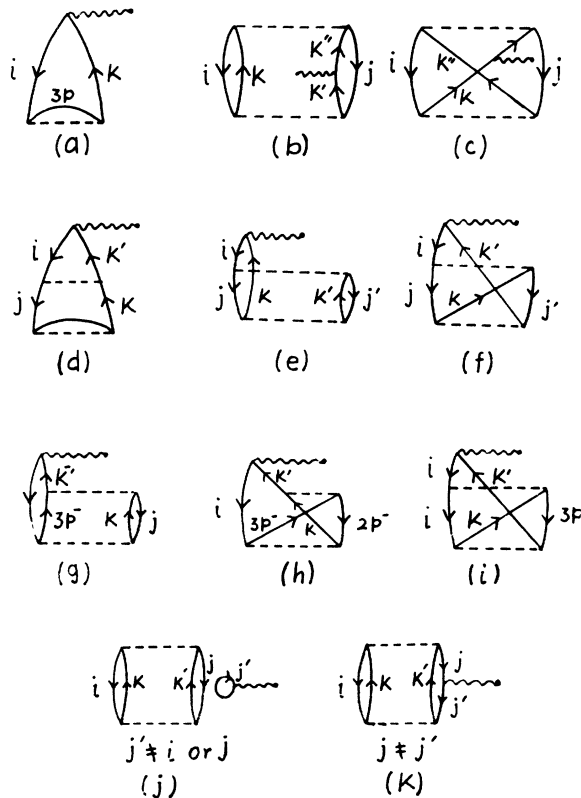


FIG. 1. Hfs diagrams for phosphorus. Only those diagrams which make major contributions to the hfs constant are presented.

that between  $3p$  and  $2s$  or  $1s$ . This is a result of the stronger overlap between  $3s$  and  $3p$  orbitals. Correspondingly,  $3p$  and  $2p$  correlate significantly because of the angular character. The total contribution from the diagrams 1(b) and 1(c) is 19.662 Mc/sec. In addition, there are twenty-some other diagrams which produced a total contribution of  $-4.987$  Mc/sec. Among these, in particular, are contributions from the unlinked diagrams, Fig. 1(j), and the nondiagonal hole-hole diagrams, Fig. 1(k), plus their respective exchange counterparts. Considerable numerical cancellation occurs among these diagrams and their sum is only  $-0.618$  Mc/sec in our case. Moreover, the individual values of these 1(j) and 1(k) diagrams are quite small and do not exceed 2.4 Mc/sec. The net result from the (1, 1) diagrams is 14.674 Mc/sec.

Of the (0, 2) diagrams, Fig. 1(d) really represents higher order effects associated with core polarization. Thus, the first two rows of Table I for this class of diagrams represent the indirect core polarization of the  $2s$  electron by the  $3p$  electron mediated by  $3s$  and  $2p$  states, respec-

tively. The other two rows represent consistency effect combined with core polarization. For example, the third row describes the effect of the exchange interaction between the  $3p$  electrons, while one of them is core polarizing the  $1s$  state. The next class of (0, 2) diagrams are those indicated in Figs. 1(e) and 1(f). The former represents effects of correlation between  $3p$  and  $3s$  states of a different nature than in 1(b). Figure 1(f) is the exchange counterpart of 1(e). Figure 1(g) represents the influence of the correlation between  $3s^+$  and  $3s^-$ , which will vanish by spin cancellation except for the fact that  $3p^-$  state is not occupied while  $3p^+$  state is. Thus, 1(g) is a residue diagram, as is also 1(h), which represents the correlation effect between  $2p^-$  and  $3s^-$  and  $2p^-$  and  $2s^-$  states. The greater contribution from  $2p^-$  and  $2s^-$  states relative to the  $3s^-$  state can be understood by the substantial overlap between states of the same principal quantum number. The last important (0, 2) diagram is 1(i) which, in the language of earlier literature,<sup>6,8,12</sup> is an exclusion-principle-violating diagram. It results from our choice of  $v^{N-1}$  potential. In both (0, 2) as well as (1, 1) diagrams, hole-hole ladder corrections are applied to  $1s$ ,  $2s$ , and  $2p$  hole lines wherever necessary. Hole-particle ladder corrections, which are more difficult to calculate and usually smaller,<sup>8,12</sup> have been neglected. In addition to the (0, 2) diagrams shown in Fig. 1, there are ninety-nine other diagrams which contribute 4.364 Mc/sec as compared with 95.352 Mc/sec from diagrams 1(d)-1(i).

Thus the (1, 1) and (0, 2) diagrams lead to the combined positive contribution of 114.390 Mc/sec, which overwhelms the negative core-polarization contribution. However, it is more appropriate to combine diagram 1(d) with diagram 1(a) since the former represents higher order effects of consistency combined with core polarization. The total core-polarization contribution then adds up to  $-52.384$  Mc/sec, while correlation effect contribution is 102.179 Mc/sec. With either of these processes of combining the diagrams, we get for the theoretical hfs constant  $A = 49.795$  Mc/sec. The remaining difference of 5.261 Mc/sec could arise from several sources. Thus, we have neglected hole-particle and particle-particle ladder corrections in both (1, 1) and (0, 2) diagrams as well as higher diagrams. Experience with these effects in lighter atoms,<sup>6-8,10</sup> particularly nitrogen, indicates that these sources could provide a substantial part of the remaining 5.261

Table I. Contributions from various hfs diagrams.

Order	Diagram	Description	Contribution (Mc/sec)
(0,1)	1(a)	i = 1s	-111.342
		i = 2s	145.620
		i = 3s	-98.874
	Total		-64.596
(1,1)	1(b)	i = 3s, j = 3p	3.017
		i = 2p, j = 3p	4.321
	1(c)	i = 3s, j = 3p	9.885
		i = 2p, j = 3p	2.438
Other (1,1)			-4.987
	Total		14.674
(0,2)	1(d)	i = 2s, j = 3s	-4.118
		i = 2s, j = 2p	13.693
		i = 1s, j = 3p	-35.959
		i = 2s, j = 3p	38.595
	1(e)	i = 3s, j = 3p, j' = 3s	23.310
	1(f)	i = 3s, j = 3p, j' = 3s	35.025
	1(g)	i = 3s, j = 3s	-14.636
	1(h)	i = 2s	29.106
		i = 3s	-18.792
	1(i)	i = 1s	-2.712
		i = 3s	31.839
Other (0,2)			4.365
	Total		99.716
	Grand total		+49.795
	Experiment		+55.055 691 ± 0.000 008

Mc/sec. Secondly, there could be significant contributions of the right order from relativistic effects. It should be remarked that the type of relativistic effects involved here is different from that usually associated with the direct contribution from valence electrons,<sup>13</sup> which is zero in the present case. Instead, we are concerned with the influence of relativistic effects on the contribution of the core *s* electrons through their core polarizations and correlations with the valence electrons. A proper treatment of such effects would require a BG many-body formalism in terms of Dirac theory.

In conclusion, it has been demonstrated that core-polarization effects in phosphorus have definite physical origin and meaning. Secondly, they are dominated by correlation effects of opposite sign, which restore agreement with experiment. Finally, the BG formalism permits a convenient and reliable procedure for calculation of both these effects. It would be desirable to test if the conclusions obtained here concerning the importance of correlation effects can also be arrived at by other many-body procedures such as the Bethe-Goldstone method, which has been applied successfully<sup>14</sup> in the past to other atoms.

Further, it would be interesting to apply the BG procedure to study other atoms such as arsenic and antimony, which have similar  $np^3$  valence configurations as nitrogen and phosphorus, as well as transition-metal atoms<sup>15</sup> like manganese and iron, where the net core-polarization contribution is small because of strong cancellations between various core  $s$  states.

\*Work supported by the National Science Foundation.

<sup>1</sup>J. M. Pendlebury and K. F. Smith, Proc. Phys. Soc. (London) **84**, 849 (1964).

<sup>2</sup>R. H. Lambert and F. M. Pipkin, Phys. Rev. **128**, 198 (1962).

<sup>3</sup>N. Bessis, H. Lefebvre-Brion, C. M. Moser, A. J. Freeman, R. K. Nesbet, and R. E. Watson, Phys. Rev. **135**, A588 (1964).

<sup>4</sup>J. Goldstone, Proc. Roy. Soc. (London), Ser. A **239**, 267 (1957).

<sup>5</sup>C. Matsubara, N. C. Dutta, Robert T. Pu, and T. P. Das, Bull. Am. Phys. Soc. **13**, 373 (1968).

<sup>6</sup>E. S. Chang, Robert T. Pu, and T. P. Das, Phys. Rev. **174**, 1, 16 (1968).

<sup>7</sup>J. D. Lyons, Robert T. Pu, T. P. Das, and E. S. Chang, Bull. Am. Phys. Soc. **12**, 1116 (1967).

<sup>8</sup>P. Bagus and A. J. Freeman, Bull. Am. Phys. Soc. **13**, 481 (1968)

<sup>9</sup>N. C. Dutta, C. Matsubara, R. T. Pu, and T. P. Das, to be published.

<sup>10</sup>E. S. Chang, thesis, University of California, Riverside, 1967 (unpublished).

<sup>11</sup>P. G. H. Sandars, in *La Structure Hyperfine des Atomes et des Molecules*, edited by R. Lefebvre and C. Moser (Editions du Centre National de la Recherche Scientifique, Paris, 1967), p. 111.

<sup>12</sup>H. P. Kelly, in *Perturbation Theory and its Application in Quantum Mechanics*, edited by C. H. Wilcox (John Wiley & Sons, Inc., New York, 1966), p. 215; Phys. Rev. **131**, 604 (1963), and **136**, B896 (1964).

<sup>13</sup>H. B. G. Casimir, *On the Interaction Between Atomic Nuclei and Electrons* (W. H. Freeman & Co., San Francisco, 1963); C. Schwartz, Phys. Rev. **105**, 173 (1956); P. G. H. Sandars and J. Beck, Proc. Roy. Soc. (London), Ser. A **289**, 97 (1965); Y. Bordarier, B. R. Judd, and M. Klapisch, Proc. Roy. Soc. (London), Ser. A **289**, 81 (1965); T. P. Das, L. Tterlikkis, and S. D. Mahanti, Phys. Rev. (to be published), and Bull. Am. Phys. Soc. **13**, 891 (1968).

<sup>14</sup>R. K. Nesbet, in *La Structure Hyperfine des Atomes et des Molecules*, edited by R. Lefebvre and C. Moser, (Editions du Centre National de la Recherche Scientifique, Paris, 1967), p. 87.

<sup>15</sup>R. E. Watson and A. J. Freeman, Phys. Rev. **123**, 2027 (1961); P. Bagus and B. Liu, Phys. Rev. **148**, 79 (1966).

## EXACT COMPUTATION OF THE VAN DER WAALS CONSTANT FOR TWO HYDROGEN ATOMS\*

Michael O'Carroll and Joseph Sucher

Center for Theoretical Physics and Department of Physics and Astronomy  
University of Maryland, College Park, Maryland

(Received 19 August 1968)

An exact formula is obtained for  $C_{HH}$ , the van der Waals constant which appears in  $V_{HH} = -C_{HH}/R^6$ , the London potential for two hydrogen atoms. Numerical evaluation gives  $C_{HH} = 6.499\,026\,7 \pm 0.000\,000\,4$ .

The London potential acting between two neutral atoms  $A$  and  $B$ ,  $V_{AB}(R) = -C_{AB}/R^6$ , is of central importance in the theory of atomic interactions at low energies. As a consequence, approximate computations of the van der Waals constant  $C_{AB}$  have been carried out for a variety of atoms over a period of many years.<sup>1</sup> The purpose of this note is to show that for the case of two hydrogen atoms, the prototype of all atom-atom interaction problems, an exact computation of  $C_{HH}$  is possible. We present below an analytic formula for  $C_{HH}$ , from which a highly accurate numerical value is readily obtained.

$C_{HH}$  may be written as the sum of a bound-state contribution  $C_{HH}^{(b)}$  and a continuum contribution  $C_{HH}^{(c)}$ :

$$C_{HH} = C_{HH}^{(b)} + C_{HH}^{(c)}, \quad (1a)$$

where

$$C_{HH}^{(b)} = -\frac{2}{3}e^4 \sum_{n=2}^{\infty} P(2W_1 - W_n)R_n \quad (1b)$$

and

$$C_{HH}^{(c)} = \frac{2}{3}e^4 \int_{-W_1}^{\infty} \frac{dw}{\pi} P(-w + W_1) \text{Im}P(w + W_1). \quad (1c)$$

Here  $W_n = -\alpha^2 m/2n^2$  ( $n = 1, 2, \dots$ ) are the bound-state energies,  $P(E)$  is defined, for complex  $E$ , by

$$P(E) = \langle \varphi_0 | \hat{x} \cdot (E - H)^{-1} \hat{x} | \varphi_0 \rangle, \quad (2)$$